Benzene-1,3-dicarboxylic acid 2,5-dimethylpyrrole derivatives as multiple inhibitors of bacterial Mur ligases (MurC–MurF)

ARTICLE *in* BIOORGANIC & MEDICINAL CHEMISTRY · JUNE 2014

Impact Factor: 2.79 · DOI: 10.1016/j.bmc.2014.05.058 · Source: PubMed

6 AUTHORS, INCLUDING:

Andrej Perdih
National Institute of Chemistry
44 PUBLICATIONS **440** CITATIONS
SEE PROFILE

Martina Hrast
University of Ljubljana
17 PUBLICATIONS **73** CITATIONS
SEE PROFILE

Gerhard Wolber
Freie Universität Berlin
145 PUBLICATIONS **2,763** CITATIONS
SEE PROFILE

Tom Solmajer
National Institute of Chemistry
98 PUBLICATIONS **1,244** CITATIONS
SEE PROFILE

Bioorganic & Medicinal Chemistry 22 (2014) 4124–4134

Contents lists available at ScienceDirect

Bioorganic & Medicinal Chemistry

journal homepage: www.elsevier.com/locate/bmc

Benzene-1,3-dicarboxylic acid 2,5-dimethylpyrrole derivatives as multiple inhibitors of bacterial Mur ligases (MurC–MurF)

Andrej Perdih [a,b,*], Martina Hrast [c], Hélène Barreteau [d], Stanislav Gobec [c], Gerhard Wolber [b], Tom Solmajer [a]

[a] National Institute of Chemistry, Hajdrihova 19, 1001 Ljubljana, Slovenia
[b] Institute of Pharmacy, Freie Universität Berlin, Königin Luise-Strasse 2+4, 14195 Berlin, Germany
[c] Faculty of Pharmacy, University of Ljubljana, Aškerčeva 7, 1001 Ljubljana, Slovenia
[d] Enveloppes Bactériennes et Antibiotiques, IBBMC, UMR 8619 CNRS, Univ Paris-Sud, 91405 Orsay, France

ARTICLE INFO

Article history:
Received 10 April 2014
Accepted 23 May 2014
Available online 2 June 2014

Keywords:
Bacterial Mur (MurC–MurF) ligase
Structure-based pharmacophores
Virtual screening
Molecular docking
Molecular dynamics (MD)
Linear Interaction Energy (LIE) method
Antibacterial agents
Drug design

ABSTRACT

Enzymes catalyzing the biosynthesis of bacterial peptidoglycan represent traditionally a collection of highly selective targets for novel antibacterial drug design. Four members of the bacterial Mur ligase family—MurC, MurD, MurE and MurF—are involved in the intracellular steps of peptidoglycan biosynthesis, catalyzing the synthesis of the peptide moiety of the Park's nucleotide. In our previous virtual screening campaign, a chemical class of benzene-1,3-dicarboxylic acid 2,5-dimethylpyrrole derivatives exhibiting dual MurD/MurE inhibition properties was discovered. In the present study we further investigated this class of compounds by performing inhibition assays on all four Mur ligases (MurC–MurF). Furthermore, molecular dynamics (MD) simulation studies of one of the initially discovered compound **1** were performed to explore its geometry as well as its energetic behavior based on the Linear Interaction Energy (LIE) method. Further in silico virtual screening (VS) experiments based on the parent active compound **1** were conducted to optimize the discovered series. Selected hits were assayed against all *Escherichia coli* MurC–MurF enzymes in biochemical inhibition assays and molecules **10**–**14** containing benzene-1,3-dicarboxylic acid 2,5-dimethylpyrrole coupled with five member-ring rhodanine moiety were found to be multiple inhibitors of the whole MurC–MurF cascade of bacterial enzymes in the micromolar range. Steady-state kinetics studies suggested this class to act as competitive inhibitors of the MurD enzyme towards D-Glu. These compounds represent novel valuable starting point in the development of novel antibacterial agents.

1. Introduction

In the last decade, the bacterial resistance to the available antibiotics has stimulated the discovery of novel efficacious antibacterial agents taking into consideration previously unexploited targets.[1,2] An essential component of bacterial cells—bacterial peptidoglycan—is traditionally a target of choice with respect to selective toxicity.[3–5] The biosynthetic pathway of bacterial peptidoglycan is a complex process divided into an initial intracellular assembly of *uridine* diphosphate (UDP)-Mur*N*Ac-pentapeptide (Park's nucleotide), followed by a translocation phase across the cell membrane and final incorporation into emerging biopolymer structure.[3–5] Peptidoglycan provides the necessary rigidity and strength that are essential for the bacterial cells to survive the high internal osmotic pressure.[3] Four members of the ADP-forming bacterial ligase family—MurC, MurD, MurE and MurF—are involved in the intracellular steps of the peptidoglycan assembly, catalyzing the synthesis of the peptide moiety by consecutive addition of L-Ala, D-Glu, *meso*-A_2pm (or L-Lys) and dipeptide D-Ala-D-Ala to the corresponding UDP-precursors.[3–5]

The Mur ligase family of enzymes represents a model example of modular structure in protein architecture, with molecules made

Abbreviations: ESP, electrostatic potential; GAFF, generalized AMBER force field; LIE, Linear Interaction Energy method; LRF, local reaction field; MD, molecular dynamics; RMSD, root-mean square distance; SAR, structure–activity relationship; SCAAS, surface constraint all atoms solvent; UDP, uridine-5′-diphosphate; UMA, uridine-5′-diphosphate-*N*-acetylmuramoyl-L-alanine; UMAG, uridine-5'-diphosphate-*N*-acetylmuramoyl-L-alanine-D-glutamate; UMT, uridine-5′-diphosphate-*N*-acetylmuramoyl-L-alanine-D-glutamate-2,6-diaminopimelic acid; VS, virtual screening.

* Corresponding author. Tel.: +386 1 4760 376; fax: +386 1 4760 300.
E-mail address: andrej.perdih@ki.si (A. Perdih).

http://dx.doi.org/10.1016/j.bmc.2014.05.058
0968-0896/

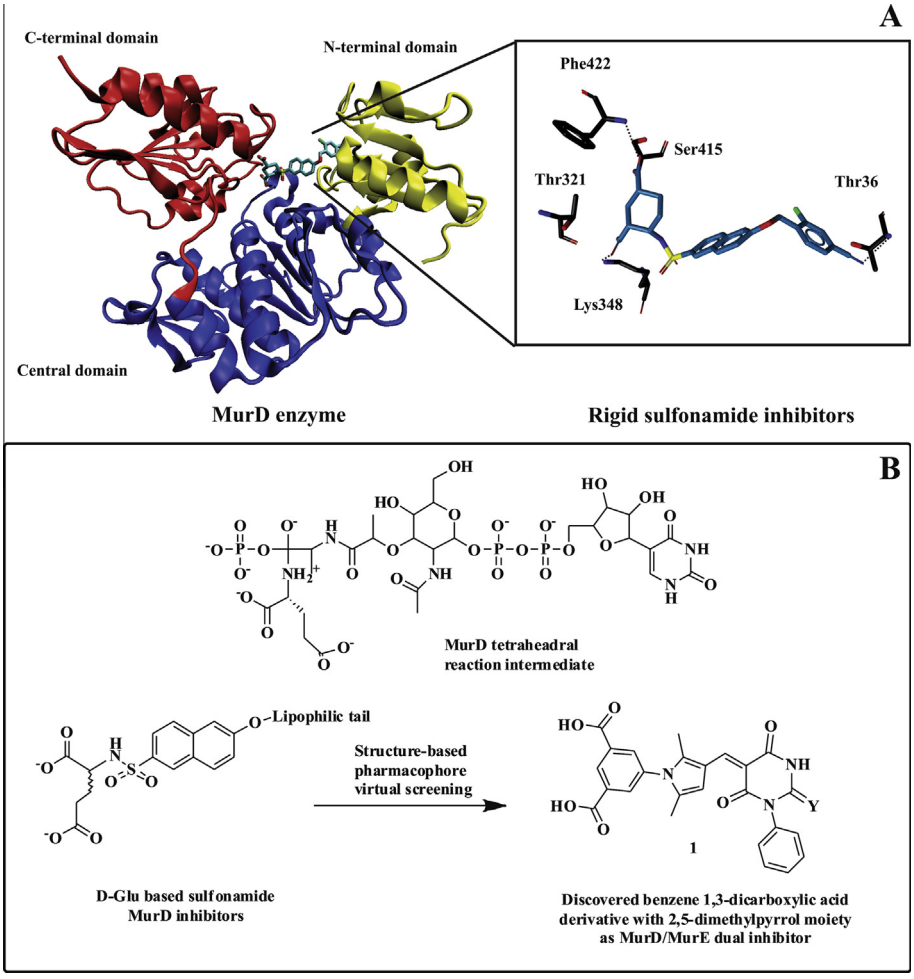

Figure 1. (A) Crystal structure of the *E. coli* MurD enzyme in complex with a representative structure of the newly discovered class of rigid sulfonamide MurD inhibitors (PDB code: 2XPC).[21] N-terminal domain is denoted in yellow, central domain in blue and C-terminal domain in red. Bound conformation of the inhibitor is located between the UDP-substrate (UMA) and the D-Glu binding site. Scheme of the most important interacting residues between the rigid sulfonamide and MurD active site[21] (B) Structures of the MurD tetrahedral reaction intermediate and structure of D-Glu-based MurD inhibitor from which compound **1** (benzene 1,3-dicarboxylic acid derivative with 2,5-dimethylpyrrole moiety) possessing dual MurD and MurE inhibitory activity was derived.[20]

up of three domains allowing for specific molecular recognition of each individual UDP-substrate.[5] The three-domain structure of these enzymes comprise an N-terminal domain responsible for binding the UDP-substrate, a central domain bearing resemblance to the nucleotide-binding domains of a number of ATP- or GTP-ases, and finally a C-terminal domain, which is involved in the binding of the incoming amino acid (or dipeptide).[3,5] Structural investigations of the Mur ligases have resulted in the identification of several distinct conformations of the enzymes, suggesting that the whole family encompasses a collection of highly complex dynamic protein targets.[5–8] All Mur ligases presumably act through an analogous sequential enzymatic mechanism, as corroborated by structural,[9] biochemical[10,11] and computational studies.[12] In the proposed mechanism, the bound UDP-precursor initially reacts with the ATP molecule yielding an acyl-phosphate intermediate,[13,14] which, after the addition of the incoming amino acid (or dipeptide), affords the tetrahedral reaction intermediate.[10,12] Finally, a dissociation of the phosphate group results in the new UDP-precursor elongated by the condensed amino acid.[10]

The Mur ligase family has already been investigated as a group of attractive emerging drug targets and several novel classes of inhibitors of these enzymes were discovered.[3,15,16] A frequently used starting point in the design of MurD enzyme inhibitors[3c] was the hypothetical structure of the MurD tetrahedral reaction intermediate.[3c,16] (Fig. 1) From this starting point, several low-molecular-weight analogues of the MurD tetrahedral intermediate structure were discovered, typically classified as derivatives of D-glutamic acid.[17] Crystal structures of the MurD enzyme complexed with these compounds have provided binding modes of several inhibitors from this class (Fig. 1A).[17] Binding free energies calculated by Linear Interaction Energy (LIE) approach revealed non-polar van der Waals interactions as the main driving force responsible for productive binding of these compounds.[18,19] Based on the available MurD crystal structures co-crystallized with *N*-sulfonyl glutamic acid inhibitors (Fig. 1B), a virtual screening campaign was performed, combining three-dimensional structure-based pharmacophores and molecular docking calculations. A novel class of glutamic acid surrogates—benzene-1,3-dicarboxylic acid derivatives—was identified: among them, compound **1** with incorporated 2,5-dimethylpyrrole moiety was found to possess dual MurD and MurE inhibitory activity.[20] In a subsequent optimization, *N*-sulfonyl glutamic acid inhibitors were also replaced with several rigid substitutes (e.g., cyclohexane- or benzene-based dicarboxylic acids) while concurrently preserving the N-substituted sulfonamide moiety.[21] These compounds showed MurD inhibition and structural studies confirmed that the compound containing cyclohexane with two carboxylic groups, acting as a rigid replacement of the D-Glu functionality, occupied the

same position as the D-Glu moiety of D-Glu inhibitors in the MurD active site[21] (see Fig. 1A for binding of one of the discovered compounds from this class of rigid sulfonamide inhibitors and its observed H-bond interaction pattern; see also Supplementary material Figs. 1S and 2S for structural alignment of several novel MurD structures and comparison with previous compounds).[15,21] Also the computed binding free energies were consistent with our previous findings that non-polar van der Waals interactions represent the main driving force responsible for binding.[19] Recently, a D-Glutamic acid-containing dual inhibitor of MurD and MurE ligases from *Escherichai coli* and *Staphylococcus aureus*, possessing promising antibacterial activity against *S. aureus* and its methicillin-resistant strain (MRSA) was described and its binding was characterized by structural studies[21b]

In the present study, further investigations of our previously discovered 2,5-dimethylpyrrole class of benzene-1,3-dicarboxylic acids[20] exhibiting dual MurD/MurE inhibition properties were performed. Molecular dynamics (MD) simulation studies of the compound **1** were initiated to explore the geometry as well as energetic behavior of its proposed binding mode in the MurD binding site with an established Linear Interaction Energy (LIE) method. In addition, further in silico virtual screening (VS) experiments using available derivatives of the parent active compound **1** were performed to expand the initial structure–activity relationships (SAR) of the series. Selected hits were assayed against all *E. coli* MurC–MurF enzymes and a steady-state kinetic study on the most promising compound on the MurD enzyme was performed. Finally, classical analogue-based medicinal chemistry approach was used to expand the SAR of this novel series.

2. Results and discussion

2.1. Evaluation of 2,5-dimethylpyrrole-based derivatives against MurC–MurF ligases and further development of the produced in silico models

A first step in further optimization of the series of previously discovered benzene-1,3 dicarboxylate 2,5-dimethylpyrrole-based derivatives **1**–**7**, all containing a six-membered dihydropyrimidine-4,6-dione moiety[20], was the evaluation of their potential inhibition on the remaining two Mur ligases, MurC and MurF from *E. coli* (Table 1). To exclude possible non-specific (promiscuous) inhibition, all compounds were tested in the presence of a detergent (0.005% Triton X-114).[22] Several compounds (**3**, **4** and **7**) not discussed in our initial screening[20] were added to the series (see Supplementary material for the origin of compounds and vendors' quality control procedures). As evident from Table 1, the compounds from this class act predominately as MurE inhibitors, as determined in our previous study with compound **1** displaying also MurD inhibition. The MurE inhibition values are located in the interval between 80 and 300 μM. In addition, compound **4** with incorporated 2-fluoro-benzene moiety displayed inhibition of the MurF enzyme with an IC_{50} value of 344 μM. Similarly, 62% residual activity at the same concentration was shown for the 4-bromobenzene derivative **7** when tested on MurC enzyme. These data hinted that this compound class might inhibit even wider range of Mur ligases compared to the initially observed dual MurD/MurE inhibition. Selected active compound **1** was also tested for its in vitro antibacterial activity against three pathogenic bacterial strains: ATCC 29213 from *S. aureus*, ATCC 29212 from *Enterococcus faecalis* and ATCC 49766 from *Haemophilus influenzae* using the protocol described in the Supporting material (see Section 8 and Table 6S). The obtained minimum inhibitory concentrations (MICs) against all three strains were higher than 128 μg/mL.

Next, in silico computational experiments using established drug design approaches were conducted to explore the observed behavior of these compounds at the atomic level. In our initial virtual screening campaign,[20] Catalyst software[23] was used as a pharmacophore-based virtual screening engine to screen libraries of commercially available compounds. The newly integrated screening engine within LigandScout[24] platform which was used in the initial study[20] only to derive structure-based pharmacophores, which were subsequently used in Catalyst for virtual screening, was validated. The conformations of the hit molecules were aligned[25] to the LigandScout pharmacophore in the same manner with this screening engine as the hit conformations identified by the Catalyst software (see Supplementary material Fig. 3S). The discriminatory performance of the derived pharmacophore model using LigandScout software was further successfully assessed using the Decoyfinder software (see Section 4).[26]

Table 1
Results of in vitro biological assays* of selected compounds **1**–**7** from benzene-1,3 dicarboxylate 2,5-dimethylpyrrole class with included substituted dihydropyrimidine-4,6-dione moiety against *E. coli* MurC–MurF ligases

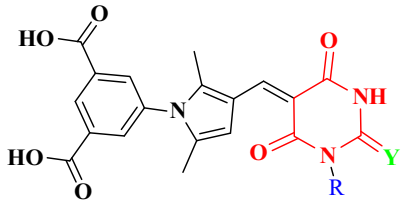

Compound	R	Y	IC_{50} (MurC)	IC_{50} (MurD)	IC_{50} (MurE)	IC_{50} (MurF)
1	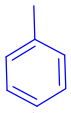	**S**	75%	690 μM**	89 μM**	84%
2	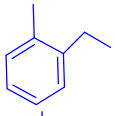	**S**	85%	92%**	55%**	68%
3	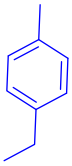	**O**	74%	81%	330 μM	75%
4	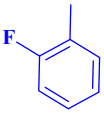	**S**	60%	71%	311 μM	344 μM
5	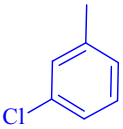	**S**	80%	90%**	104 μM**	78%
6	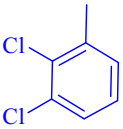	**S**	96%	83%**	79 μM**	86%
7	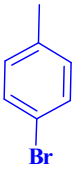	**O**	62%	71%	211 μM	60%

* Residual activities in % were determined at 250 μM concentration of the investigated compound.
** Inhibition data published previously in Ref. 20 for MurD and MurE inhibition.

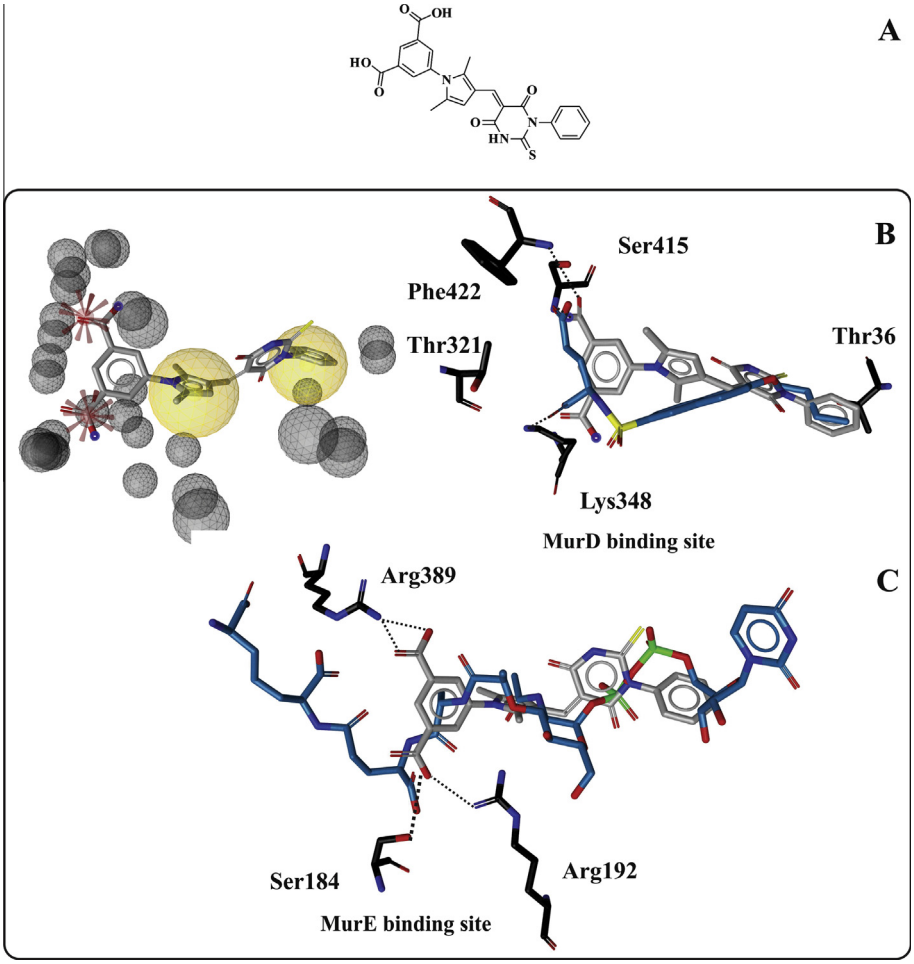

Figure 2. (A) Chemical structure of the dual MurD/MurE inhibitor **1**, (B) (left) conformation of the virtual hit **1** aligned to LigandScout structure-based pharmacophore using LigandScout as a screening engine. Yellow spheres represent hydrophobic areas and red stars negative ionic interactions. Exclusion volume spheres (grey spheres) represent the derived spatial restraints of the MurD binding site (right) GOLD-calculated binding pose of the VS hit compounds **1** docked into the MurD (PDB code: 2JFF) binding site along selected MurD residues, (C) GOLD-calculated binding pose of the VS hit compounds **1** docked into MurE (PDB code: 1E8C) binding site along with experimental position of the UMT MurE product and along with selected MurE residues.

In our initial virtual screening campaign, Catalyst-identified hit compounds were docked into the *E. coli* MurD active site (see Fig. 2B for the observed network of hydrogen bonds) using GOLD molecular docking package.[17,20,27] In these docking experiments, it was determined that the benzene-1,3 dicarboxylic moiety of these compounds occupied the same position as the D-Glu moiety in the MurD active site, acting as its rigid surrogate displaying the same hydrogen bonds interaction pattern.[20] Recent structural studies on the rigid D-Glu-based derivatives confirmed that such rigid moieties can indeed occupy the D-Glu-binding site.[21]

For the MurE enzyme from *E. coli*, only a crystal structure with the end product uridine-5′-diphosphate-*N*-acetylmuramoyl-L-alanine-D-glutamate-2,6-diaminopimelic acid (UMT) is available (PDB:1E8C) and the exact placement of the D-Glu moiety in the MurE incoming uridine-5′-diphosphate-*N*-acetylmuramoyl-L-alanine-D-glutamate (UMAG) substrate is not known.[28] Structural alignment of the MurD and MurE enzymes revealed that these two enzymes share a well preserved ATP-binding domain and similar position of the C-terminal domains (see superposition of MurD/MurE enzyme in the Supplementary material, Fig. 5S).[28] In the MurE crystal structure, D-Glu moiety of the UMT product interacts through its α-carboxylic group with Arg192, Ser184, Thr157 and Thr158 MurE residues (see Fig. 5S for the UMT interaction with MurE).

In addition to the MurD-bound conformation, we also opted to construct the putative binding model of these molecules in the MurE binding site[20] as compounds **1**–**7** displayed predominantly inhibition activity on this bacterial enzyme. Results of the docking calculations are depicted in Figure 2C for the most frequently appearing docking solution. In addition, the experimentally determined position of the UMT product in the 1E8C structure is shown. The most frequently occurring docking results displayed that benzene 1,3-dicarboxyilic moiety of compound **1** is placed in the vicinity of the UMT D-Glu moiety (Fig. 2C). In addition, the hydrogen bonds between Arg192, Ser184 and the first carboxylic group of the benzene-1,3 dicarboxylic moiety were observed which mimic the D-Glu α-carboxylic group interaction in UMT with MurE. The second carboxylic group interacts with MurE Arg389 residue which also interacted with the part of the UMT in the reported crystal structure (see Fig. 5S). The remaining portion of compound **1** stretches in the MurE pocket toward the uridine binding site. This comparison provided further rationalisation for the observed behaviour of several glutamic acid-based compounds; nevertheless a caveat must be stated that in the absence of structural data this determined position is still subject to a certain degree of uncertainty.

In order to provide further insight into the binding of 2,5-dimethylpyrrole class of Mur ligases inhibitors, molecular dynamics

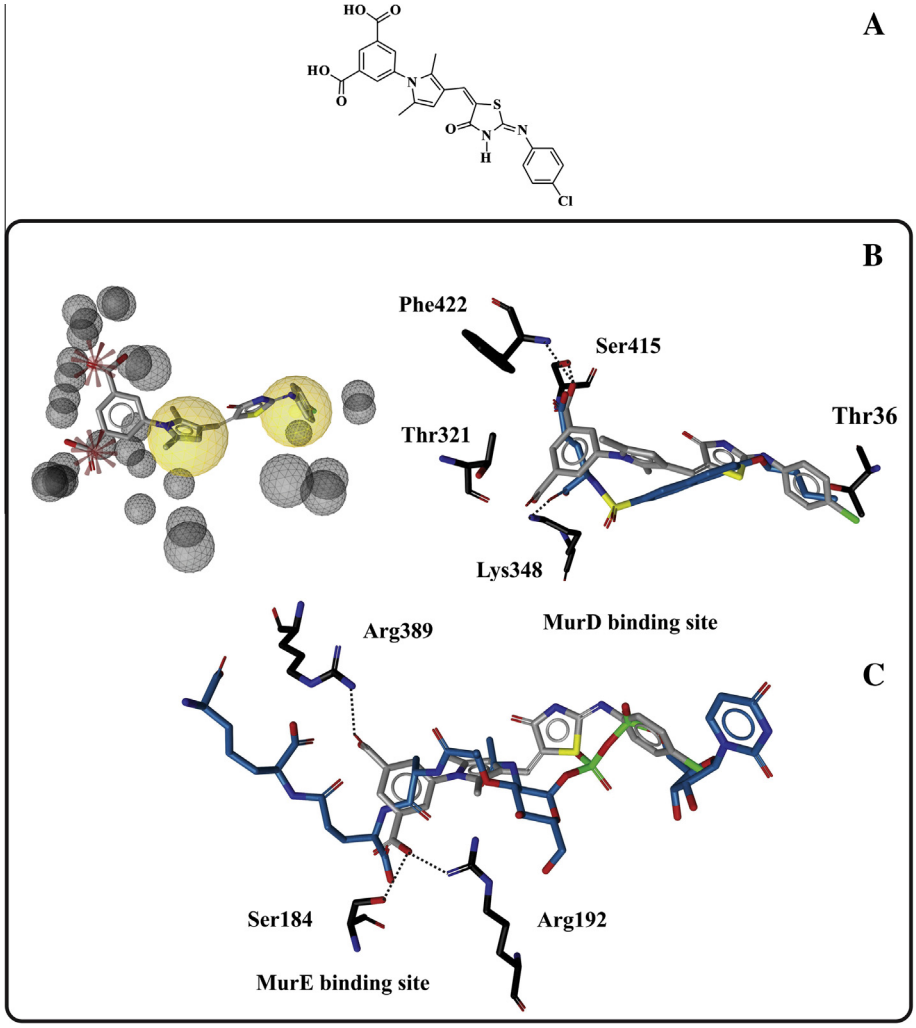

Figure 3. (A) Chemical structure of the hit compound **13**, (B) (left) conformation of the virtual hit **13** aligned to LigandScout structure-based pharmacophore using LigandScout as a screening engine. Yellow spheres represent hydrophobic areas and red stars negative ionic interactions. Exclusion volume spheres (grey spheres) represent the derived spatial restraints of the MurD binding site (right) GOLD-calculated binding pose of the VS hit compounds **13** docked into the MurD (PDB code: 2JFF) binding site long selected MurD residues, (C) GOLD-calculated binding pose of the VS hit compounds **13** doked into MurE (PDB code: 1E8C) binding site along with selected MurE residues.

(MD) simulations were initiated for the docked conformation of inhibitor **1** in the *E. coli* MurD active site accompanied by Linear Interaction Energy (LIE) calculations.[29] Experimental structural data supporting the use of the initial binding mode was provided by the structural studies of the rigid MurD inhibitors containing a dicarboxylic cyclic moiety (see Fig. 1A and Supplementary material, Figs. 1S and 2S).[21] In Supplementary material, Section 7, a full description of the methodology and detailed discussion of the obtained MD/LIE results is provided. We also present the animation of the calculated MD trajectory for this compound in the bound state. The MD results confirmed the stability of the ligand **1** binding mode in the MurD binding site and further analysis displayed a preserved network of hydrogen bonds between ligand **1** and the MurD binding site. Energetic aspect of the molecular recognition was subsequently addressed by calculating interaction energies between ligand **1** and its surroundings (for both investigated states: free state and bound state) using program Q.[30] The results were in line with our previous observations[18,19] that revealed non-polar interactions as the predominant driving force for the binding of this inhibitor, with electrostatics playing a minor role. We also determined the binding free energy using LIE coefficients ($\alpha = 0.176$ $\beta = 0.06$) derived in our previous free energy studies of the inhibitors designed within the D-Glu paradigm with similar binding modes.[18,19] It was gratifying to observe that compound **1** behaved in a similar fashion as previously studied compounds and the calculated binding free energy was determined within the general rule of chemical accuracy.[31] Overall these results in the absence of structural data for this class have provided us with some more confidence for subsequent optimization design steps.

2.2. Virtual screening and experimental evaluation of novel compounds from 2,5-dimethylpyrrole class against MurC–MurF ligases

The encouraging results after performing inhibition assays of our benzene-1,3 dicarboxylic acid 2,5-dimethylpyrrole class of dual MurD/MurE ligase inhibitors (see Section 2.1) stimulated us to design an additional virtual screening campaign utilizing our previously derived pharmacophore model, containing two negative ionisable areas to model the negatively charged electrostatic features of the carboxylic groups, together with two hydrophobic interaction spheres, reflecting the lipophilic characteristics of the inhibitors.[20] We were especially interested in finding optimization possibilities for the six-membered dihydropyrimidine-4,6-dione moiety attached to the rigid benzene-1,3 dicarboxylic acid

2,5-dimethylpyrrole core, which was retained during this optimization. A large-scale virtual screening campaign was performed by screening our new library of approximately 6.0 million commercially available compounds against this pharmacophore model. This library of virtual compounds was prepared as described in the Section 4. The compounds were aligned to the investigated pharmacophore using the alignment method available in the LigandScout program. The virtual screening campaign yielded approximately 600 hit compounds and an example of the identified hit molecule **13**—benzene-1,3-dicarboxylic acid 2,5-dimethylpyrrole coupled with a five member-ring rhodanine moiety—which showed potential to serve as a dihydropyrimidine-4,6-dione replacement is shown of Figure 3B.

Obtained Ligandscout hits were subsequently docked into the MurD and MurE active sites using GOLD molecular docking package. It has to be noted that MurC and MurF enzymes, although their apoenzymes are available[5], were not used in docking studies due the fact that in the case of Mur ligases we are dealing with large binding sites which pose a substantial difficulty to rationally set up the calculations and subsequently perform meaningful validation of results. In this respect, the MurE model reported here represents the first attempt based on the structural work by Gordon et al.[28] Moreover, significant observed conformational motion of the protein domains (C-terminal and N-terminal) that can occur even with ligand binding makes such computational endeavours even more challenging and outmost care is required at every new step.[5] Future structural studies will eventually enable the utilization of MurC and MurF structures as well.

Active sites of the MurD and MurE enzymes were prepared as described in the Section 4. The obtained binding geometries were visually inspected for all hit compounds. The class of compounds that showed similar behaviour as compounds described in Section 2.1, in terms of binding to MurD and MurE active sites represented compounds where five member-ring rhodanine moiety was attached to the initial benzene-1,3-dicarboxylic acid 2,5-dimethylpyrrole moiety. The first ranked conformations for the representative compound **13** in Figure 3B and C can be easily compared with the previous class, depicted in Figure 2. The selected compounds **8**–**14** were assayed in our standard Malachite green assays against all four Mur ligases (MurC–MurF) enzymes (see Supplementary material for the origin of these compounds and vendors' quality control procedures). Non-specific (promiscuous) inhibition, a problem with some compounds containing the rhodanine moiety, was excluded as all compounds were again tested in the presence of a detergent.[22] Results of the inhibition assay are presented in Table 2.

It was gratifying to observe that compounds **10**–**14** showed multiple inhibition of all four Mur ligases (MurC–MurF) and the best compound within the series—compound **13**—inhibited the ligases in the low micromolar range. By analyzing inhibition data in Table 2, it seems that introduction of the substituents at the *para* position contributed favorably to the inhibition activity on all four Mur ligases. Similar values were observed for the bromine derivative **14**, whereas a methoxy and aliphatic substitutions (compounds **10**–**12**) gave higher inhibition values on all four ligases. In terms of MurD inhibition, an approximately 10-fold stronger MurD inhibition over the initial compound **1** (IC_{50} (MurD) = 690 μM) was observed by our reutilization of the previously derived structure-based pharmacophore. These compounds are to the best of our knowledge the first inhibitors of all four MurC–MurF ligases where IC_{50} values were determined for all four enzymes and were found to inhibit the whole family in the micromolar range. To provide some initial SAR regarding the importance of benzene moiety at the R1 position, compound **9** that has no benzene substituent was rendered as completely inactive. Similar observation was detected in our initial study for the first 2,5-dimethylpyrrole class of inhibitors described in Section 2.1.[20] Interestingly, its structurally very similar compound **8** with incorporated sulfur at the R1 position displayed inhibition against three Mur ligases MurC–MurE. It should be also noted that substituted 5-benzylidenethiazolidin-4-ones without included benzene-1,3-dicarboxylic acid 2,5-dimethylpyrrole moiety were already shown to be promising inhibitors of the bacterial Mur ligases MurD–MurF in low micormolar range and for some compounds of this class promising residual activities on MurC enzyme were determined as well. In comparison with our compounds these compounds showed better MurD–MurF inhibition profile, while for the MurC the IC_{50} values were not determined what hinders the possibility for a full comparison.[21c]

Table 2
Results of in vitro biological assays* of novel compounds **8**–**14** from the benzene-1,3 dicarboxylate 2,5-dimethylpyrrole class with included substituted rhodanine moiety against MurC–MurF ligases

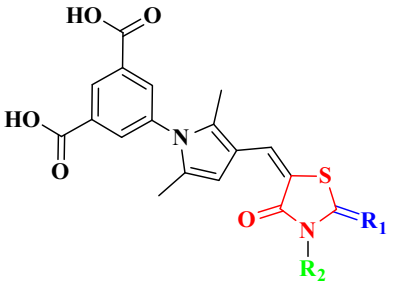

Compound	R1	R2	IC_{50} (MurC)	IC_{50} (MurD)	IC_{50} (MurE)	IC_{50} (MurF)
8	S	**H**	133 μM	95 μM	406 μM	89%
9		**CH_3**	106%	89%	97%	95%
10	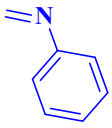	**H**	205 μM	206 μM	494 μM	298 μM
11	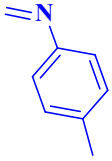	**H**	107 μM	170 μM	245 μM	201 μM
12	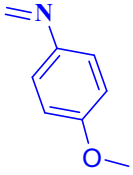	**H**	172 μM	168 μM	303 μM	281 μM
13	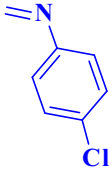	**H**	41 μM	60 μM	93 μM	89 μM
14	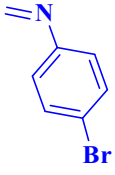	**H**	44 μM	66 μM	89 μM	102 μM

* Residual activities in % were determined at 250 μM concentration of the investigated compound.

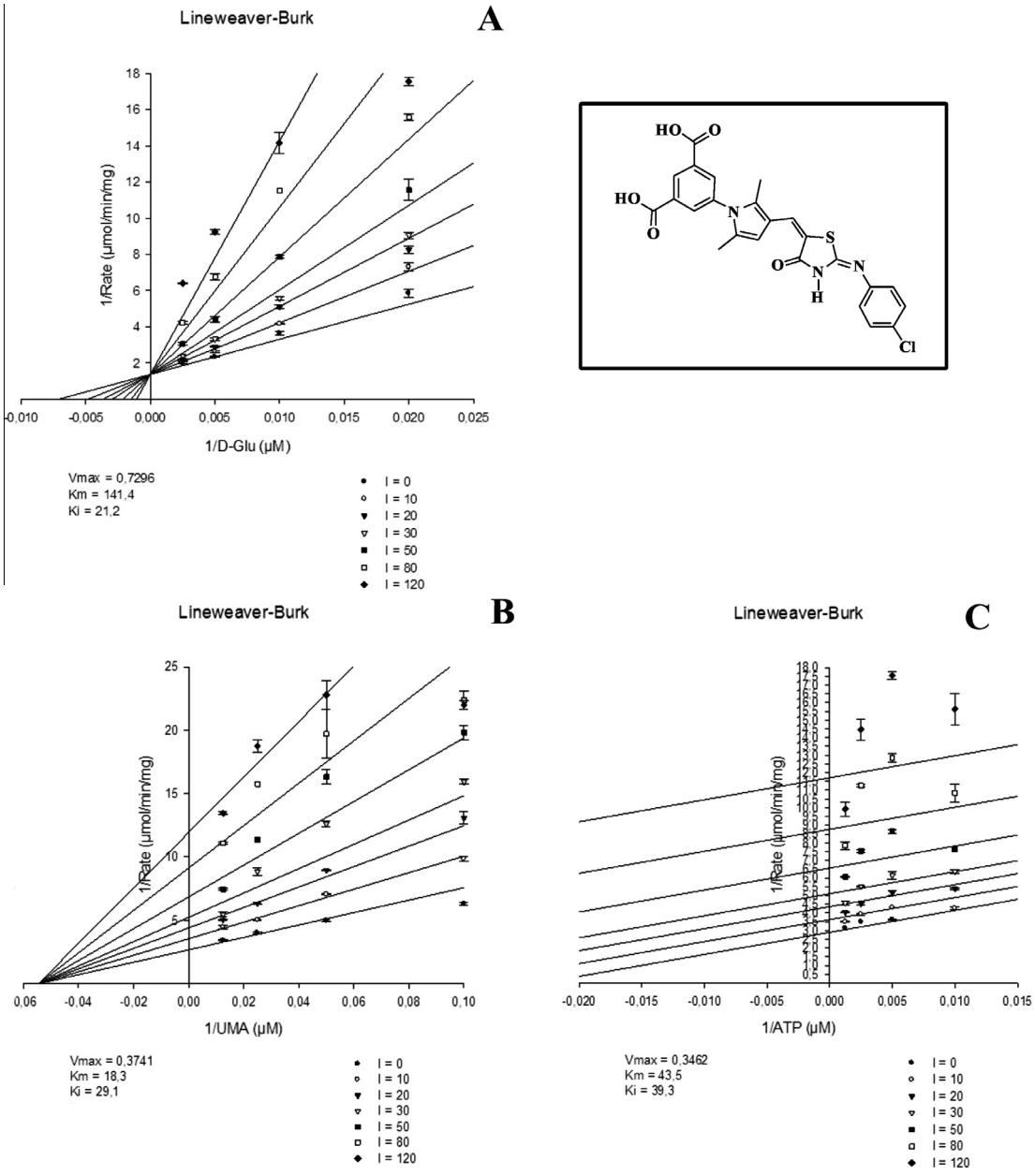

Figure 4. Steady-state kinetics of the interaction between MurD and compound **13**. Data were collected for compound **13** versus (A) D-Glu (80 µM UMA, 400 µM ATP), (B) UMA (100 µM D-Glu, 400 µM ATP), (C) ATP (100 µM D-Glu, 80 µM UMA). For clarity, the data points shown are average values of the two data sets; the standard deviation was within ±10% of the average value.

Selected active compounds **8** and **10** from this class were also tested for their in vitro antibacterial activity against the same three pathogenic bacterial strains as previously tested compound **1** (see Supplementary material, Table 6S). The minimum inhibitory concentration (MICs) of compound **8** against *E. faecalis* was found to be around 128 µg/mL. In all other cases values higher than 128 µg/mL were determined. Further studies will have to concentrate their efforts on finding molecules that will on one hand fulfill this promising pharmacophore pattern and on the other hand have superior physical–chemical properties that will enable efficient compound penetration into the bacterial cell giving rise to increased antibacterial activity.

In order to get a more in depth mechanistic insight into the inhibition mechanism of the newly discovered compounds, steady-state kinetics were performed for the most active compound 13 on the MurD enzyme. In our previous work, the obtained apparent K_M values for each substrate ($K_{M,app,UMA}$ = 6.0 ± 0.8 µM, $K_{M,app,D\text{-}Glu}$ = 95 µM ± 9 and $K_{M,app,ATP}$ = 90 ± 7 µM) were fully in line with other values in the lit.,[3c,17] The resulting best model revealed a mode of inhibition of compound **13** as a competitive inhibitor with respect to D-Glu, (Fig. 4, Table 3). The determined K_i value of 21 ± 2 µM was in good agreement with the IC_{50} value on MurD obtained in the standard MurD screening assay and the correlation of IC_{50} and K_i values was so far observed also for other compounds within the D-Glu based compounds.[17,21] The produced

Table 3
Inhibitory properties of compound **13** against all three MurD natural ligands (D-Glu, ATP; UMA)

Substrat	Inhibition mechanism	K_i (µM)	R^2
D-Glu	Competitive	21 ± 2	0.973
ATP	Uncompetitive (partial)	39 ± 6	0.949
UMA	Non-competitive (partial)	29 ± 3	0.969

Table 4
Results of the in vitro biological assays* of selected compounds **15–21** against MurC–MurF ligases form *E. coli*. Compounds were selected to investigate the influence of the benzene-1,3-dicarboxylic acid 2,5-dimethylpyrrole moiety on the overall ligase inhibitory activity.

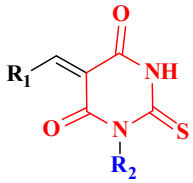

Compound	R1	R2	IC_{50} or RA at 250 μM (MurC)	IC_{50} or RA at 250 μM (MurD)	IC_{50} or RA at 250 μM (MurE)	IC_{50} or RA at 250 μM (MurF)
15	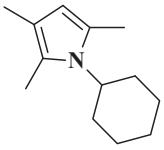	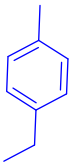	92%	100%	97%	75%
16	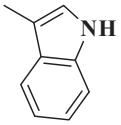	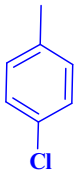	77%	71%	44 μM	20%
17	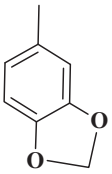	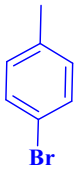	120%	91%	81%	95%
18	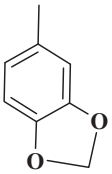	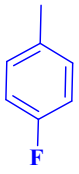	108%	102%	97%	81%

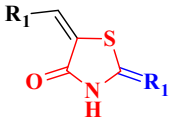

Compound	R1	R2	IC_{50} or RA at 250 μM (MurC)	IC_{50} or RA at 250 μM (MurD)	IC_{50} or RA at 250 μM (MurE)	IC_{50} or RA at 250 μM (MurF)
19	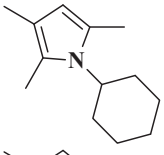	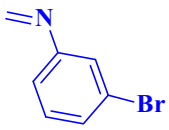	89%	79%	91%	93%
20	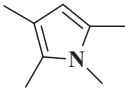	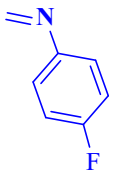	82%	78%	76%	67%
21	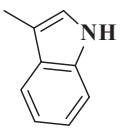	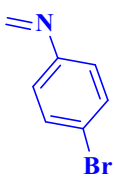	87%	102%	90%	75%

* Residual activities given in % were determined at 250 μM concentration of the investigated compound.

best models of inhibition with respect to UMA showed partial non-competitive inhibition, and with respect to ATP partial uncompetitive inhibition, however with less favourable statistics of the obtained models and higher K_i values (Table 3). This data provides crucial support of the binding models for this series on the MurD enzyme.

Despite the fact that these observations offer some important early insights into the binding of the novel discovered class of MurD inhibitors, these observations cannot be directly transferred to binding properties of these compounds to other Mur ligase enzymes. In addition, the observed conformational flexibility of the family poses an additional challenge to describe the positions from the available data. We hope that these issues can be fully addressed in our future studies.

Structural information about the binding of our discovered compounds to the members of the Mur ligase family (MurC–MurF) are currently still not available despite intensive efforts (see Acknowledgment section for our collaborators on structural studies). As we wanted to further expand the knowledge about SAR requirements for binding, we resorted to a classical SAR analogues-based medicinal chemistry approach.[32] For this purpose, derivatives from both classes of inhibitors discussed in this study were further investigated by evaluating the selected analogues **15**–**21**. When selecting these compounds we took into account our previous SAR information that revealed the presence of the benzene moiety attached to the heterocycle (five-membered or six-membered) is generally required for the inhibition activity and that its *para* substitution contributes favorably.

Selected compounds **15**–**18** from the first dihydropyrimidine-4,6-dione class of inhibitors were selected predominantly with the purpose of exploring the importance of the dicarboxylic moiety present, or the benzene dicarboxylate function in general. In compounds **16**–**18** the benzene dicarboxylic functionality was completely omitted and furthermore 2,5-dimethylpyrrole was replaced with different moieties available in the databases. Compounds were screened against all four *E. coli* Mur ligases (MurC–MurF) and obtained results are presented in Table 4. In all cases apart from compound **16** where MurE inhibition was still present (IC_{50} = 44 μM) along with quite potent inhibition of MurF (RA = 20% at 250 μM), compounds were rendered as inactive. Compound **16** contains a 1*H*-indole heterocycle which could play a role in inhibition activity on these two enzymes. Nevertheless, investigated compound **18** which contained all elements apart from dicarboxylic moiety was shown to be completely inactive. This speaks in favour of the benzene dicarboxylic functionality as well as the 2,5-dimethylpyrrole moiety for the successful Mur ligase inhibition results.

Even more crucial for further insight into the influence of multiple Mur ligase inhibition capacity represented compounds **19**–**21** where the importance of benzene dicarboxylic functionality was investigated in comparison to the active compounds **10**–**14**. All compounds were rendered as inactive suggesting that the benzene dicarboxylic functionality is essential for inhibition. Interestingly, compound **21** containing indole heterocycle present in compound **16** did not show any activity on MurE and MurF ligases.

3. Conclusions

In this study, we further investigated the benzene-1,3-dicarboxylic acid 2,5-dimethylpyrrole class of dual MurD/MurE inhibitors discovered in our previous virtual screening campaign.[20] Initial screening of the expanded series on all four Mur ligases (MurC–MurF) showed prospects for expanding the inhibition on all ligases. Molecular dynamics (MD) simulation studies of one of the originally discovered compound **1** was initiated to explore the geometry and energetic behavior in the MurD active site using the Linear Interaction Energy (LIE) method and applying LIE coefficients derived in our previous studies of MurD inhibitors.[18,19] Compound **1** displayed in all aspects behavior typically observed for the compounds designed within the D-Glu paradigm.

Additional in silico virtual screening (VS) experiments based on the parent active compound **1** were conducted to optimize the discovered series. Selected hits were assayed against all MurC–MurF enzymes in inhibition assays. Novel molecules **10**–**14** containing benzene-1,3-dicarboxylic acid 2,5-dimethylpyrrole coupled with the five member-ring rhodanine moiety were found to be multiple inhibitors of the whole cascade of Mur ligases (MurC–MurF) in the low micromolar range. Furthermore, steady-state kinetics studies of compound **13** suggested that molecules from this class act as competitive inhibitors of the MurD enzyme towards D-Glu. Finally, by using a classical analogue-based medicinal chemistry approach, a presence of the benzene dicarboxylic moiety along with benzene-based substitution of the five or six-membered heterocyclic moiety were shown as prerequisites for multiple Mur ligase inhibition properties.

Compounds **10**–**14** represent a novel class of multiple inhibitors of all four Mur ligases and as such provide new evidence of the earlier assumptions that inhibition of the whole ligase enzymatic cascade is possible.[3,5,21c] We hope that these compounds will serve the research community interested in antibacterial drug design as novel promising leads that could by further optimization pave the way to promising novel antibacterial agents.

4. Materials and methods

4.1. Structure-based pharmacophore modeling and virtual screening

In our previous virtual screening campaign, three dimensional structure-based pharmacophore model was derived based on the available structural information about the binding of the D-Glu based inhibitors using LigandScout pharmacophore generator.[20,24] Performed alignment of newly available crystal structures containing rigid and other D-Glu-based MurD inhibitors[15,21] showed the same pharmacophore features as observed previously for the novel D-Glu based compounds (see also Supplementary material Figs. 1S and 2S for structural alignment of the available MurD structures[15,17,21] as well as alignment of the derived structure-based pharmacophores).

Our initial virtual screening campaign[20] used Catalyst software[23] as a pharmacophore-based virtual screening engine to screen libraries of commercially available compounds. The newly available screening engine within LigandScout[24] platform, used in the initial study[20] only to derive structure-based pharmacophores was now validated to establish if Catalyst hit compounds could also be identified using LigandScout as a pharmacophore virtual screening engine. Compounds **1**–**7** were converted into the Ligandscout multiconformer form (100 conformations per molecule) and screened against previously derived structure-based pharmacophore and result is presented in Figure 2 for compound **1**. The conformation of the hit molecule was aligned[25] to the LigandScout pharmacophore in the same manner as the hit conformation identified by the Catalyst software (see Supplementary material Fig. 3S for overlay comparison). The discriminatory performance of the derived pharmacophore model was further validated by a screening experiment against 100 decoy molecules generated for active compounds **1** using the Decoyfinder software.[26] Decoyfinder generates sets of decoy molecules for defined active ligands. Decoys have similar number of rotational bonds, hydrogen bond acceptors, hydrogen bond donors, log*P* value and molecular weight as active molecules but are chemically different, which is defined by a maximum Tanimoto value threshold between active ligand and decoy

molecule MACCS fingerprints.[26] The pharmacophore model successfully identified the active compound in the correct orientation and none of the generated decoy molecules were identified as potential hits.

The pharmacophore model was used to screen approximately 6.0 million commercially available compounds, all of which were beforehand converted into multiconformer format (25 conformers for each compound in the database) using the LigandScout screening module. The conformers of the molecules in the screening library were generated using the idbgen module that is available in the Ligandscout, coupled with the OMEGA software.[33] The default high-throughput settings were used for the library generation: maximum number of output conformers per molecule = 25; RMS threshold to duplicate conformers = 0.8 Å; maximum number of all generated conformers per molecule = 30,000; and maximum number of intermediate conformers per molecule = 4000. In the virtual screening experiments, each compound had to fulfill all of the derived pharmacophore constraints to be identified as a virtual hit. Pharmacophore Fit scoring function available in LigandScout was used to score the matching of the hit molecules to the pharmacophore model, LigandScout screening procedure retrieved approximately 600 hit compounds that were carefully visually assessed to identify compound classes not identified in the previous virtual screening campaign.

4.2. Molecular docking calculations

Pharmacophore hits obtained in the virtual screening campaign using Ligandscout were subsequently docked into the MurD enzyme active site using GOLD molecular docking package.[27] Protein structure 2JFF was used to construct the MurD active site, which was defined around experimental coordinates of the bound inhibitor in the 2JFF structure, resulting in a cavity radius of 13.3 A.[20] Each molecule was docked 10 times into the binding site by applying the following parameters of the GOLD genetic algorithm (GA) (Population size = 100, Selection pressure = 1.1, No. of Operations = 100,000, No. of Islands = 5, Niche Size = 2, Migrate = 10, Mutate = 95, Crossover = 95). Early termination was allowed if the top 3 solutions were within 1.5 Å of the RMSD value and GOLD score available scoring function was used as it showed to be more applicable to our system.[20] The quality of the generated binding poses, as well as the scoring function assessment were validated[34] by redocking the original compound (see Supplementary material for details Fig. 4S) as well as on a set of 20 D-Glu inhibitors, (*N*-sulfonyl and *N*-carbonyl derivatives), where the available structural data permitted a satisfactory validation procedure[20]

Obtained pharmacophore hits of the novel virtual screening procedure were docked into the MurE active site also using the GOLD molecular docking engine.[27] MurE protein structure (PDB code: 1E8C)[28] from *E. coli* co-crystallized with the enzymatic product UMT was used to construct the MurE active site, which was defined within the radius of 10 Å around experimental coordinates of the UMT product in the 1E8C MurE structure. Again each molecule was docked 10 times into the binding site by applying the following parameters of the GOLD genetic algorithm (GA) (Population size = 100, Selection pressure = 1.1, No. of Operations = 100,000, No. of Islands = 5, Niche Size = 2, Migrate = 10, Mutate = 95, Crossover = 95). Early termination was allowed if the top 3 solutions were within 1.5 Å of the RMSD value.

4.3. Biological assays of inhibition of MurC–MurF ligases from *E. coli*

The inhibition of Mur ligases from *E. coli* was determined using the Malachite green assay with slight modifications.[3a,b,35,36] The mixture with final volume of 50 μL contained:

MurC: 50 mM Hepes, pH 8.0, 5 mM $MgCl_2$, 0.005% Triton X-114, 120 μM L-Ala, 120 μM UM, 450 μM ATP, purified MurC from *E. coli* and 250 μM of each tested compound dissolved in DMSO.

MurD: 50 mM Hepes, pH 8.0, 5 mM $MgCl_2$, 0.005% Triton X-114, 100 μM D-Glu, 80 μM UMA, 400 μM ATP, purified MurD from *E. coli* and 250 μM of each tested compound dissolved in DMSO.

MurE: 50 mM Hepes, pH 8.0, 15 mM $MgCl_2$, 0.005% Triton X-114, 60 μM mDAP, 100 μM UMAG, 1000 μM ATP, purified MurE from *E. coli* and 250 μM of each tested compound dissolved in DMSO.

MurF: 50 mM Hepes, pH 8.0, 50 mM $MgCl_2$, 0.005% Triton X-114, 600 μM D-Ala-D-Ala, 100 μM UMtri-mDAP, 500 μM ATP, purified MurF from *E. coli* and 250 μM of each tested compound dissolved in DMSO.

In all cases, the final concentration of DMSO was 5% (v/v). After incubation for 15 min at 37 °C, the enzyme reaction was terminated by adding Biomol® reagent and the absorbance was measured at 650 nm. All of the experiments were run in duplicate. Residual activities (RAs) were calculated with respect to similar assays without the tested compounds and with 5% DMSO. The IC_{50} values, which were determined by measuring the residual activities at seven different compound concentrations, represented the concentration for which the RA was 50%.

Example compounds **1** and **13** from each discovered benzene-1,3 dicarboxylate 2,5-dimethylpyrrole class of inhibitors were characterized, and their purity was determined by microanalysis performed on a Perkin-Elmer C, H, N, S analyzer using a modified Pregl–Dumas method. The purity of the tested compound was established to be ⩾95% (see Supporting information, Section 2).

4.4. Kinetic analysis of the inhibition of the MurD enzyme by compound 13

For compound **13**, K_i values were determined against MurD from *E. coli*. K_i determinations were performed under similar conditions as described for MurD inhibition assay, where different concentrations of one substrate and fixed concentrations of the other two were used.[17] First, the concentration of ATP (100, 200, 400 and 800 μM) was varied at fixed concentrations of UMA (80 μM) and D-Glu (100 μM), then the concentration of UMA (10, 20, 40 and 80 μM) was changed at fixed concentrations of ATP (400 μM) and D-Glu (100 μM), and finally, the concentration of D-Glu (50, 100, 200 and 400 μM) was modified at fixed concentrations of ATP (400 μM) and UMA (80 μM). The concentrations of compound **13** were 0, 10, 20, 30, 50, 80 and 120 μM. After 15 min of incubation, 100 μL of Biomol green reagent was added, and absorbance was read at 650 nm after 5 min. Initial data were fitted to competitive, non-competitive and uncompetitive inhibition models in which v is observed reaction rate, V the maximum rate and K_M the Michaelis constant, using SigmaPlot 12.0 software. The best fit was taken as the one having the highest R^2, the lowest standard error and the narrowest 95% confidence interval in each parameter (see Table 3).

Acknowledgments

This work was supported by the Ministry of Education, Science and Sport of the Republic of Slovenia through Post-doctoral Project Grant number: Z1-4111 and the applied research Project Grant number L1-4039. The authors would like thank Dr. Jernej Zidar from the Institute of High Performance Computing (IHPC), Singapure, and Barbara Pogorelčnik from the National institute of Chemistry, Slovenia, for their technical assistance with LIE calculations. Dr. Sandy Favini, Dr. Carlos Contreras-Martel and Dr. Andréa Dessen from the Bacterial Pathogenicity Group at the Institut de Biologie Structurale (*IBS*), Grenoble, France, are acknowledged

and thanked for performing several structural experiments on MurD, MurE and MurF enzymes. Dr. Andreja Kovač from the Faculty of Pharmacy, University of Ljubljana, is acknowledged and thanked for performing initial inhibition assays of some of the novel compounds discussed in this work. Dr. Didier Blanot from the Université Paris-Sud, France is thanked for critical reading of the manuscript.

A. Supplementary data

Supplementary data associated with this article can be found, in the online version, at http://dx.doi.org/10.1016/j.bmc.2014.05.058. These data include MOL files and InChiKeys of the most important compounds described in this article.

References and notes

1. Silver, L. L. *Biochem. Pharmacol.* **2006**, *71*, 996.
2. (a) Brown, E. D.; Wright, G. D. *Chem. Rev.* **2005**, *105*, 759; (b) Silver, L. L. *Clin. Microbiol. Rev.* **2011**, *24*, 71.
3. (a) Vollmer, W.; Blanot, D.; de Pedro, M. A. *FEMS Microbiol. Rev.* **2008**, *32*, 149; (b) Barreteau, H.; Kovač, A.; Boniface, A.; Sova, M.; Gobec, S.; Blanot, D. *FEMS Microbiol. Rev.* **2008**, *32*, 168; (c) Šink, R.; Barreteau, H.; Patin, D.; Mengin-Lecreulx, D.; Gobec, S.; Blanot, D. *Biomol. Concepts* **2013**, *4*, 539.
4. van Heijenoort, J. *Nat. Prod. Rep.* **2001**, *18*, 503.
5. Smith, C. S. *J. Mol. Biol.* **2006**, *362*, 640.
6. Bertrand, J. A.; Fanchon, E.; Martin, L.; Chantalat, L.; Auger, G.; Blanot, D.; van Heijenoort, J.; Dideberg, O. *J. Mol. Biol.* **2000**, *301*, 1257.
7. Perdih, A.; Kotnik, M.; Hodoscek, M.; Solmajer, T. *Proteins: Struct., Funct. Bioinf.* **2007**, *68*, 243.
8. (a) Perdih, A.; Solmajer, T. *Comput. Theor. Chem.* **2012**, *979*, 73; (b) Perdih, A.; Hrast, M.; Barreteau, H.; Gobec, S.; Wolber, G.; Solmajer, T. *J. Chem. Inf. Model.* **2014**, *54*, 1451.
9. Bertrand, J. A.; Auger, G.; Martin, L.; Fanchon, E.; Blanot, D.; Le Beller, D.; van Heijenoort, J.; Dideberg, O. *J. Mol. Biol.* **1999**, *289*, 579.
10. Anderson, M. S.; Eveland, S. S.; Onishi, H.; Pompliano, D. L. *Biochemistry* **1996**, *35*, 16264.
11. Emanuele, J. J., Jr.; Jin, H.; Yanchunas, J., Jr.; Villafranca, J. J. *Biochemistry* **1997**, *36*, 7264.
12. Perdih, A.; Hodoscek, M.; Solmajer, T. *Proteins: Struct., Funct. Bioinf.* **2009**, *74*, 744.
13. Bouhss, A.; Dementin, S.; van Heijenoort, J.; Parquet, C.; Blanot, D. *Methods Enzymol.* **2002**, *354*, 189.
14. Falk, P. J.; Ervin, K. M.; Volk, K. S.; Ho, H.-T. *Biochemistry* **1996**, *35*, 1417.
15. Zoeiby, A. E.; Sanschagrin, F.; Levesque, R. C. *Mol. Microbiol.* **2002**, *47*, 1.
16. Tanner, M. E.; Vaganay, S.; van Heijenoort, J.; Blanot, D. *J. Org. Chem.* **1996**, *61*, 1756.
17. (a) Kotnik, M.; Humljan, J.; Contreras-Martel, C.; Oblak, M.; Kristan, K.; Hervé, M.; Blanot, D.; Urleb, U.; Gobec, S.; Dessen, A.; Solmajer, T. *J. Mol. Biol.* **2007**, *370*, 107; (b) Humljan, J.; Kotnik, M.; Contreras-Martel, C.; Blanot, D.; Urleb, U.; Desssen, A.; Solmajer, T.; Gobec, S. *J. Med. Chem.* **2008**, *51*, 7486.
18. Perdih, A.; Bren, U.; Solmajer, T. *J. Mol. Model.* **2009**, *15*, 983.
19. Perdih, A.; Wolber, G.; Solmajer, T. *J. Comput.-Aided Mol. Des.* **2013**, *27*, 723.
20. Perdih, A.; Kovač, A.; Wolber, G.; Blanot, D.; Gobec, S.; Solmajer, T. *Bioorg. Med. Chem. Lett.* **2009**, *19*, 2668.
21. (a) Sosič, I.; Barreteau, H.; Simčič, M.; Šink, R.; Cesar, J.; Zega, A.; Grdadolnik, S. G.; Contreras-Martel, C.; Dessen, A.; Amoroso, A.; Joris, B.; Blanot, D.; Gobec, S. *Eur. J. Med. Chem.* **2011**, *46*, 2880; (b) Tomašić, T.; Šink, R.; Zidar, N.; Fic, A.; Contreras-Martel, C.; Dessen, A.; Patin, D.; Blanot, D.; Premru-Műllerm, M.; Gobec, S.; Zega, A.; Kikelj, D.; Peterlin Mašič, L. *ACS Med. Chem. Lett.* **2012**, *3*, 626; (c) Tomašić, T.; Zidar, N.; Kovač, A.; Turk, S.; Simčič, M.; Blanot, D.; Premru-Műllerm, M.; Filipič, M.; Golič Grdadolnik, S.; Zega, A.; Anderluh, M.; Gobec, S.; Kikelj, D.; Peterlin Mašič, L. *ChemMedChem* **2010**, *5*, 286.
22. McGovern, S. L.; Stoichet, B. K. *J. Med. Chem.* **2003**, *46*, 1478.
23. Catalyst; Accelrys Software: San Diego.
24. Wolber, G.; Langer, T. *J. Chem. Inf. Model.* **2005**, *45*, 160.
25. Wolber, G.; Dornhofer, A.; Langer, T. *J. Comput.-Aided Mol. Des.* **2006**, *20*, 773.
26. Cereto-Massague, A.; Guasch, L.; Valls, C.; Mulero, M.; Pujadas, G.; Garcia-Vallve, S. *Bioinformatics* **2012**, *28*, 1662.
27. Jones, G.; Willett, P.; Glen, R. C.; Leach, A. R.; Taylor, R. *J. Mol. Biol.* **1997**, *267*, 727.
28. Gordon, E.; Flouret, B.; Chantalat, L.; van Heijenoort, J.; Mengin-Lecreulx, D.; Dideberg, O. *J. Biol. Chem.* **2001**, *276*, 10999.
29. Åqvist, J.; Medina, C.; Samuelson, J. E. *Protein Eng.* **1994**, *7*, 385.
30. Marelius, J.; Kolmodin, K.; Feierberg, I.; Åqvist, J. *J. Mol. Graph. Model.* **1998**, *16*, 213.
31. Bash, P. A.; Ho, L. L.; MacKerell, A. D.; Levine, D.; Hallstrom, P. *Proc. Natl. Acad. Sci. U.S.A.* **1996**, *93*, 3698.
32. *The Practice of Medicinal Chemistry*; Wermuth, C.-G., Ed., 3r d ed.; Academic Press, 2008.
33. (a) OMEGA 2.4.6; OpenEye Scientific Software Inc: Santa Fe, NM, 2012; (b) Hawkins, P. C. D.; Skillman, A. G.; Warren, G. L.; Ellingson, B. A.; Stahl, M. T. *J. Chem. Inf. Model.* **2010**, *50*, 572.
34. Kirchmair, J.; Markt, P.; Distinto, S.; Wolber, G.; Langer, T. *J. Comput. Aided Mol. Des.* **2008**, *22*, 213.
35. Auger, G.; Martin, L.; Bertrand, J.; Ferrari, P.; Fanchon, E.; Vaganay, S.; Petillot, Y.; van Heijenoort, J.; Blanot, D.; Dideberg, O. *Protein Expression Purif.* **1998**, *13*, 23.
36. Lanzetta, P. A.; Alvarez, L. J.; Reinach, P. S.; Candia, O. *Anal. Biochem.* **1979**, *100*, 95.